Journal of Alloys and Compounds 488 (2009) 420–424

Contents lists available at ScienceDirect

Journal of Alloys and Compounds

journal homepage: www.elsevier.com/locate/jallcom

Grain growth in Ni–Mn–Ga alloys

Franziska Thoss[a,*], Martin Pötschke[a], Uwe Gaitzsch[a], Jens Freudenberger[a], Wolfgang Anwand[b], Stefan Roth[a], Bernd Rellinghaus[a], Ludwig Schultz[a]

[a] IFW Dresden, P.O. Box 270116, D-01171 Dresden, Germany
[b] Forschungszentrum Dresden-Rossendorf, P.O. Box 510119, D-01314 Dresden, Germany

ARTICLE INFO

Article history:
Received 18 June 2009
Received in revised form 1 September 2009
Accepted 2 September 2009
Available online 8 September 2009

Keywords:
Magnetically ordered materials
Casting
Grain boundaries

ABSTRACT

The influence of annealing temperature and time on grain growth in polycrystalline Ni–Mn–Ga samples near the stoichiometric composition Ni_2MnGa was investigated. Grain growth was only observed for compositions with a Ni-content below 50 at.%. The existence of constitutional vacancies as a possible origin for the different grain growth behavior was excluded by positron annihilation spectroscopy (PAS). In order to activate grain boundary motion and hence grain growth in $Ni_{50}Mn_{29}Ga_{21}$ the samples were annealed and deformed in situ in compression up to various strain levels. A sharp threshold to initiate grain growth is observed between 8% and 10% of compressive strain.

1. Introduction

Ni_2MnGa, a magnetic shape memory alloy, is in the focus of research due to its large reversible strain, which appears at moderate external magnetic fields (<1 T) [1] and its resultant possible applications as sensors [2,3] or actuators [4,5].

The discovery of the magnetic shape memory effect in Ni_2MnGa single crystals was published in 1995 by Chernenko et al. [6] and in 1996 by Ullakko et al. [7]. Up to now, the work is mainly focused on the investigation of single crystals, because grain boundaries hinder the motion of twin boundaries. But single crystal growth is a time- and cost-consuming process. And, as the application of this material is still a primary objective, the development of cost- and time-efficient production techniques is of major interest. Novel processes like zone-melting [8] improved the homogeneity of the composition along the rod enormously compared with the usually used Bridgman method.

As another approach, casting of polycrystalline materials could provide a possible alternative. Yet, in polycrystals exhibiting an isotropic microstructure only a few well oriented grains support the magnetic field induced strain. An improvement has been achieved by textured polycrystalline samples as prepared by Pötschke et al. by directional solidification of different compositions near stoichiometric Ni_2MnGa. There, an insulated, preheated mold with a heat sink at the bottom causes a uniaxial heat flow. As a consequence a columnar grain structure is observed. In this case, the preferred growth orientation in the cubic high-temperature austenitic phase is ⟨1 0 0⟩ [9]. Furthermore, Gaitzsch et al. trained such samples mechanically to increase twin boundary mobility [10]. Thereby, the magnetic field induced strain could be increased up to 1% in $Ni_{50}Mn_{29}Ga_{21}$ [11].

In order to enhance the strain further, the microstructure of such samples can be optimized by means of grain coarsening, which is usually achieved by annealing. Here, it is to be noted that so far only in single crystals and in large grained polycrystals magnetic field induced strain is reported.

In the case of polycrystalline magnetic shape memory alloys, in particular of Ni_2MnGa samples, annealing meets a number of different demands. Primarily a special annealing procedure is necessary to develop a certain sort of the martensitic phase: 5M, 7M and NM, respectively [12]. Besides relieving internal stresses, reduction of inhomogeneities is another important goal in most heat treatments. Currently Schlagel et al. investigated a series of different annealing times for chill cast $Ni_{50}Mn_{37}Sn_{13}$ samples [13]. Annealing times of 1 h or 2 h did not suffice to dissolve the netlike segregations, but in contrast an annealing time of 72 h did. Also Yuhasz et al. showed that an extended annealing (about 4 weeks) at 1223 K is needed to gain a chemical and structural homogenization for $Ni_{50}Mn_{50-x}Sn_x$ (x = 11–15) [14].

Another interesting effect of heat treatment was investigated by Liu et al. concerning the influence on the martensitic transformation behavior in polycrystalline CoNiGa samples [15]. With decreasing annealing temperature and cooling rate, the martensitic transformation temperature also decreases, which is a matter of the composition of the two coexisting phases.

* Corresponding author. Tel.: +49 351 4659694.
E-mail addresses: f.thoss@ifw-dresden.de (F. Thoss), s.roth@ifw-dresden.de (S. Roth).

0925-8388/$ – see front matter © 2009 Elsevier B.V. All rights reserved.
doi:10.1016/j.jallcom.2009.09.003

The most important annealing effect in the present work is grain growth. For the magnetic shape memory alloy $Co_{46}Ni_{27}Ga_{27}$ the growth velocity of grains with different orientations and various local compositions (precipitates), respectively, was found to be different [16].

Hence, we investigate the influence of different annealing temperatures and times for $Ni_{48}Mn_{30}Ga_{22}$ and $Ni_{50}Mn_{29}Ga_{21}$ on grain growth. $Ni_{48}Mn_{30}Ga_{22}$ is austenitic at room temperature and therefore preferable for Electron Backscatter Diffraction (EBSD) measurements due to the absence of twin boundaries, thus allowing the microstructure to be observed directly. The grain orientation measured in the austenite transforms to a specific grain orientation in the martensite upon cooling through the transformation temperature. All of the alloys clearly show the same microstructures, consisting of radially oriented, fine grains. Thus, the grain orientation measured at room temperature for $Ni_{48}Mn_{30}Ga_{22}$ in the austenitic state is a measure for the orientation of $Ni_{50}Mn_{30}Ga_{20}$ and $Ni_{50}Mn_{29}Ga_{21}$ at room temperature in the martensitic state as long as no grain growth occurred. Consequently, the aim of this work is to study the grain growth behavior of the chosen alloys depending on the annealing temperature and time.

In order to check for possible differences in the defect concentration as origin for different grain growth behavior, positron annihilation spectroscopy (PAS) has been applied.

Finally, improving the annealing process should result in larger grains, eventually leading to an increased magnetic field induced strain in polycrystals. To initiate grain growth in samples with hindered grain boundary mobility, the samples were plastically hot deformed at the beginning of the annealing time.

2. Experimental

To obtain the desired compositions for $Ni_{48}Mn_{30}Ga_{22}$, $Ni_{49}Mn_{30}Ga_{21}$, $Ni_{50}Mn_{25}Ga_{25}$, $Ni_{50}Mn_{29}Ga_{21}$ and $Ni_{51}Mn_{29}Ga_{21}$ specific amounts of the pure elements Nickel (99.99%), Manganese (99.8%) and Gallium (99.999%) were induction-melted and cast into a copper mold (⌀20 mm, length approximately 120 mm). The rods were electroerosively cut into half cylindrical slices (thickness 4 mm). After the samples were ground (SiC-paper up to 4000) and etched (nitrohydrochloric acid), optical images of the microstructure were taken by a CCD-camera. Subsequent annealing was performed in a reducing atmosphere (Ar, 5% H_2) at various temperatures from 900 °C to 1100 °C for 48 h and 96 h, respectively.

The martensitic transformation temperature was determined by differential scanning calorimetry (DSC). The deviation of these temperatures from the expected values was less than 5 K. With the knowledge, that a composition deviation of about 0.1 at.% shifts the transformation temperature by 5 K [17], we therefore assume the samples to have the nominal composition.

For the mechanical tests, rod-shaped samples were required. For this purpose, rods were cast from the master alloy $Ni_{50}Mn_{29}Ga_{21}$ by centrifugal casting into a cold copper mold (⌀6 mm, length approximately 75 mm) and cut into cylinders of 10 mm length. The samples were annealed at 1000 °C in Ar at 22 mbar. After the samples were thermally equilibrated, they were compressed at a constant strain rate of $1 \times 10^{-4}\ s^{-1}$ until a specific total strain between 6% and 17% had been achieved. Subsequently the samples were kept at the annealing temperature for further 6 h without intermediate cooling and external load.

$Ni_{50}Mn_{29}Ga_{21}$ and $Ni_{48}Mn_{30}Ga_{22}$ samples in the as-cast state were investigated by PAS (Doppler broadening method) in order to check the concentration of structural defects. Defects like vacancies act as positron traps due to their high electron density. They are mainly surrounded by valence electrons. Since valence electrons have a lower energy than core electrons the Doppler broadening of the annihilation radiation shows different values for valence- and core electrons, respectively. The energy of the positron beam was varied in order to measure the Doppler broadening of the positron–electron annihilation energy depending on the incident positron energy and therewith depending on the sample depth. The results of positron annihilation spectroscopy can be summarized in the so-called *S*-parameter which is directly related to the defect concentration [18].

3. Results and discussion

Fig. 1 shows the typical microstructures of $Ni_{48}Mn_{30}Ga_{22}$ and the MSM-active $Ni_{50}Mn_{29}Ga_{21}$. Both alloys exhibit the same microstructure with narrow and radially oriented grains, visualizing the radial heat flow during solidification.

To investigate the influence of the annealing temperature on the microstructure, samples of both, $Ni_{48}Mn_{30}Ga_{22}$ and $Ni_{50}Mn_{29}Ga_{21}$, were annealed for 48 h at 900 °C, 1000 °C, 1050 °C and 1100 °C, respectively (Fig. 2). For both alloys annealing at 900 °C does not effect a change of the microstructure in comparison to the as-cast state (cf. Fig. 1). An increase of the annealing temperature to 1000 °C results in grain growth for $Ni_{48}Mn_{30}Ga_{22}$ (left column of Fig. 2). For an annealing temperature of 1050 °C the number of grains decreases further and, as it can be seen from the longitudinal cut, the grains capture the entire sample thickness. A heat treatment at 1100 °C results in the melting of the sample surface. The images of the right column show that the microstructure of $Ni_{50}Mn_{29}Ga_{21}$ remained unaffected by the annealing procedure. At 1100 °C partial melting is observed without previous grain growth. Evidently there is a strong difference in the grain growth behavior for the two compositions under investigation.

Since grain growth is based on diffusion, it may also depend on the annealing time. Fig. 3 shows the microstructures of $Ni_{48}Mn_{30}Ga_{22}$ and $Ni_{50}Mn_{29}Ga_{21}$, after the samples were annealed at 1000 °C for 48 h and 96 h, respectively. The increase of the annealing time did not result in an enhanced grain growth in any of the alloys. This is visible especially at the grain at the top of the sample in $Ni_{48}Mn_{30}Ga_{22}$ (cf. Figs. 2b and 3a), where size and shape of the grains did not change by doubling the annealing time. Likewise, in $Ni_{50}Mn_{29}Ga_{21}$ grain growth could not be induced by further annealing (cf. Figs. 2h and 3c).

The origin of this different grain growth behavior was to be investigated further. Besides their different compositions, these two alloys in general differ in their structure at room temperature ($Ni_{48}Mn_{30}Ga_{22}$ is austenitic and $Ni_{50}Mn_{29}Ga_{21}$ is martensitic). So, at first glance, there seem to be two possible origins for that

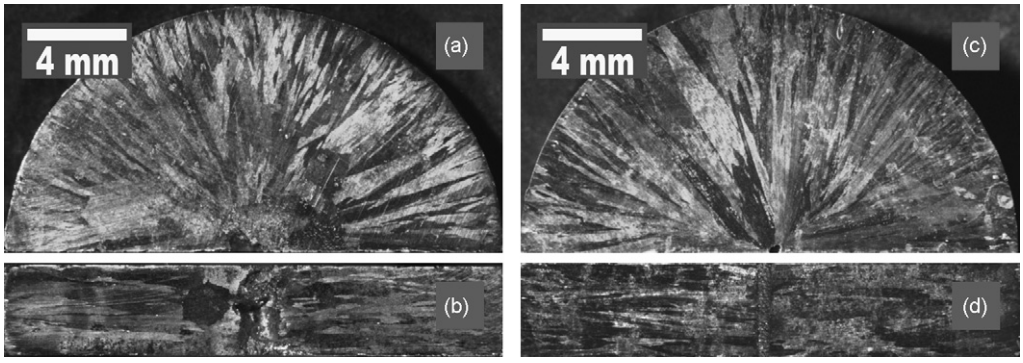

Fig. 1. As-cast microstructure of $Ni_{48}Mn_{30}Ga_{22}$ (left) and $Ni_{50}Mn_{29}Ga_{21}$ (right): (a) and (c) topviews and (b) and (d) frontviews.

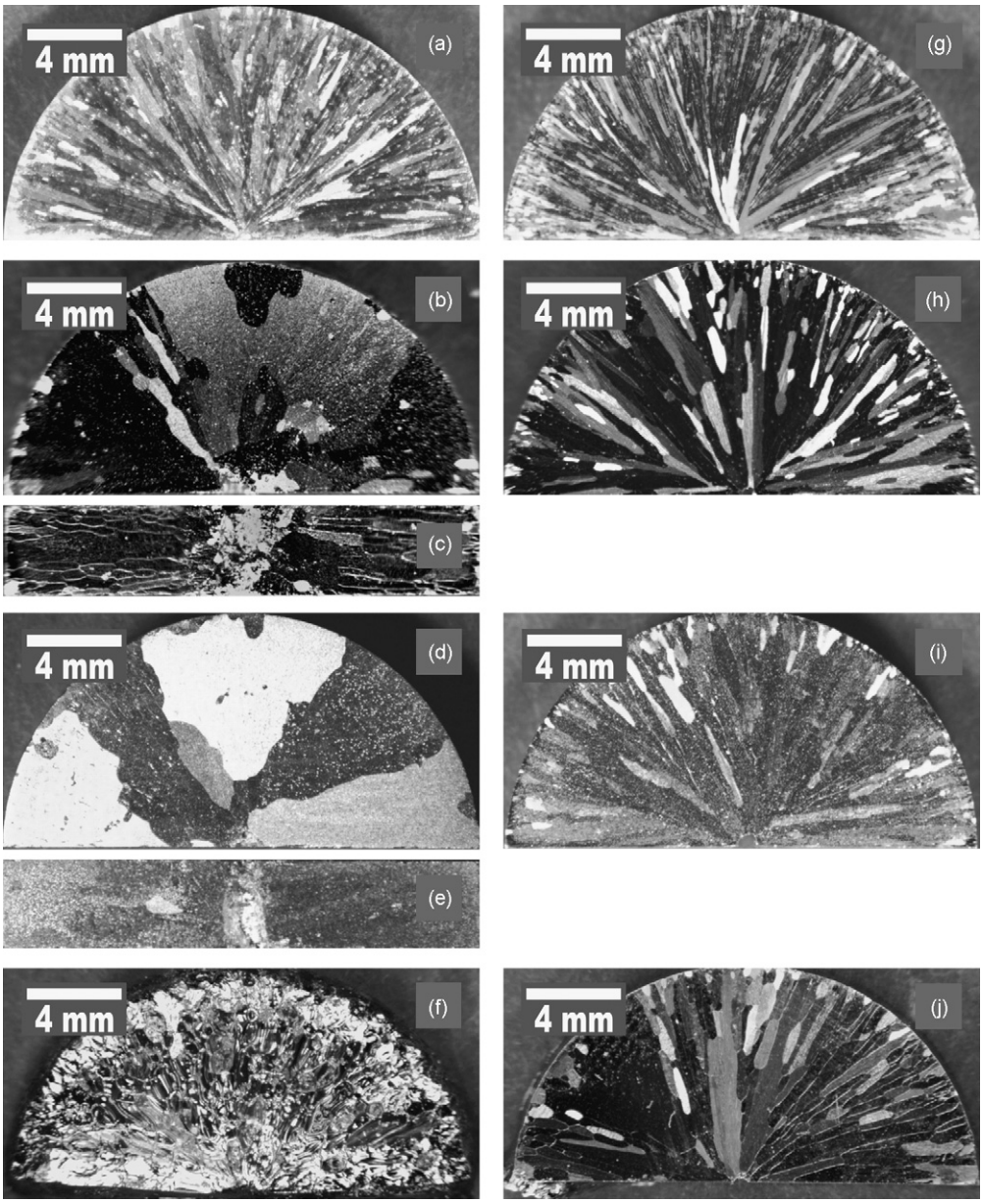

Fig. 2. Variation of the annealing temperature: microstructure of $Ni_{48}Mn_{30}Ga_{22}$ (left) and $Ni_{50}Mn_{29}Ga_{21}$ (right), (a) and (g) at 900 °C, (b) and (h) at 1000 °C, (d) and (i) at 1050 °C, (f) and (j) at 1100 °C, (c) and (e) are the frontviews of the upper pictures.

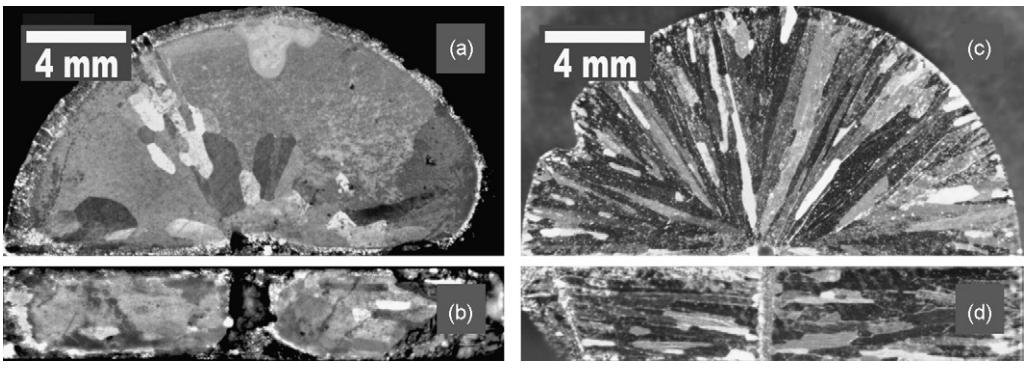

Fig. 3. Variation of the annealing time: microstructure of $Ni_{48}Mn_{30}Ga_{22}$ ((a) topview and (b) frontview) and $Ni_{50}Mn_{29}Ga_{21}$ ((c) topview and (d) frontview) after 96 h at 1000 °C, in comparison to Fig. 2.

Table 1
Annealing behavior of various alloys at 1000 °C (48 h) with regard to grain growth behavior related to Ni-content and structure at room temperature.

Structure at RT	Ni-content		
	<50 at.%	50 at.%	>50 at.%
Austenitic	$Ni_{48}Mn_{30}Ga_{22}$ grain growth	$Ni_{50}Mn_{25}Ga_{25}$ no grain growth	
Martensitic	$Ni_{49}Mn_{30}Ga_{21}$ grain growth	$Ni_{50}Mn_{29}Ga_{21}$ no grain growth	$Ni_{51}Mn_{29}Ga_{21}$ no grain growth

behavior. First, the $Ni_{50}Mn_{29}Ga_{21}$ alloy was transformed to the martensitic state during preparation which could lead to residual defects, hindering the grain boundary motion; second, an incompletely occupied Ni-sublattice (Ni-content below 50%) could result in constitutional vacancies which would enhance diffusion and thus promote grain growth. Typically, Ni–Mn–Ga alloys with compositions near Ni_2MnGa solidify in the B2-structure (CsCl-structure) with one sublattice occupied by Ni and the other sublattice occupied by Mn and Ga. Below about 750 °C such alloys transform to the $L2_1$-structure (Heusler type structure) with two sublattices occupied by Ni and the other two sublattices occupied by Mn and Ga, respectively [19]. This means, at the annealing temperature only the ratio of Ni atoms to the sum of Mn and Ga atoms and thus possible resulting Ni vacancies are of interest.

In order to identify the origin of the different grain growth behavior, additional samples were investigated: (i) a room temperature martensitic alloy with a Ni-content below 50% ($Ni_{49}Mn_{30}Ga_{21}$), (ii) a room temperature austenitic alloy with a Ni-content of 50% ($Ni_{50}Mn_{25}Ga_{25}$) and (iii) a room temperature martensitic alloy with a Ni-content above 50% ($Ni_{51}Mn_{29}Ga_{20}$). In accordance with the previous procedure these samples were annealed at 1000 °C for 48 h. Table 1 summarizes the grain growth behavior for all samples. Grain growth is observed only for samples with a Ni-content below 50%. Due to the fact, that room temperature austenitic as well as room temperature martensitic alloys exhibit grain growth, a structure transformation during preparation can be ruled out as the sole reason for the different grain growth behavior.

The correlation between the Ni-content of the samples and the occurrence of grain growth might suggest that there are empty sites in the Ni-sublattice, so-called constitutional vacancies. Such vacancies would enhance the diffusivity and thus, promote grain growth. In order to check the vacancy concentration $Ni_{48}Mn_{30}Ga_{22}$ and $Ni_{50}Mn_{29}Ga_{21}$ samples were investigated by PAS. In Fig. 4, the *S*-parameter, associated with the defect density, is plotted as a function of the positron energy, which is directly related to the information depth. Within a thin near-surface layer, i.e. for low positron energies, the *S*-parameter decreases steeply with increasing positron energy ($E_p \approx 0$–2.5 keV). The plateaus, which extend up to $E_p \approx 10$ keV, are typical for metallic samples. They arise from the

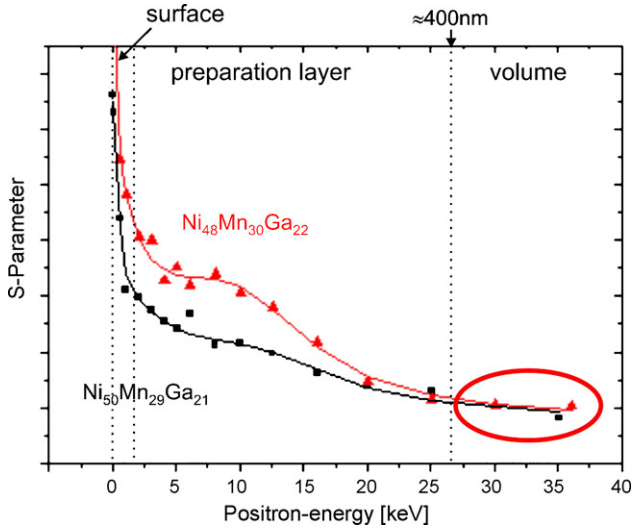

Fig. 4. Positron annihilation spectroscopy: *S*-parameter as a function of the positron energy for $Ni_{48}Mn_{30}Ga_{22}$ and $Ni_{50}Mn_{29}Ga_{21}$. Hereby, the information depth is tunable via the positron energy. The *S*-parameter (*S*: shape) is a measure for the size and concentration of defects and the $S(E)$ plot results in a defect-depth profile.

preparation layers at the surface, generated by the grinding process and characterized by an increased defect density (mainly dislocations). The plateau is located at a higher level of the *S*-parameter for the austenitic $Ni_{48}Mn_{30}Ga_{22}$ in comparison to the martensitic $Ni_{50}Mn_{29}Ga_{21}$. This is a direct consequence of the hardness, which is higher for $Ni_{50}Mn_{29}Ga_{21}$ compared to $Ni_{48}Mn_{30}Ga_{22}$ causing a more pronounced damage of the microstructure of the softer $Ni_{48}Mn_{30}Ga_{22}$ by a similar sample preparation. Apart from that, the two curves do not differ for positron energies larger than 27 keV, an energy which corresponds to a depth of about 400 nm. This result affirms that the defect density in the bulk is the same for both alloys at room temperature. Thus, constitutional vacancies can be excluded as origin of the different behavior of grain growth. This result is also supported by the work of Richard et al. [20], who found by neutron diffraction, that "excess Ni goes to Mn sites and excess

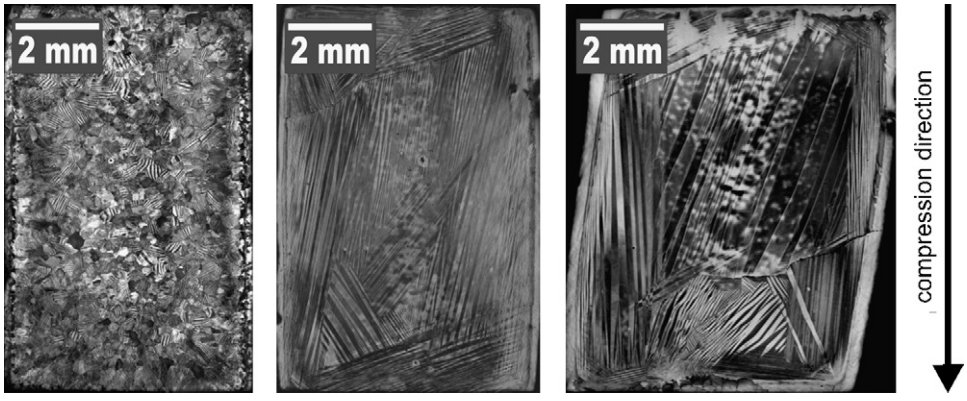

Fig. 5. Microstructures of samples with 6%, 10% and 17% compressive strain (applied at 1000 °C).

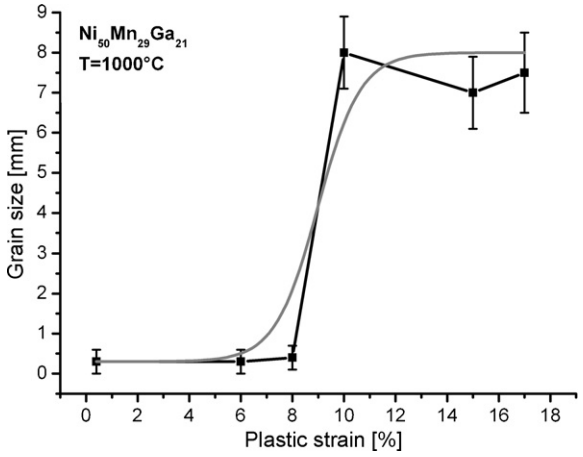

Fig. 6. Average grain size versus plastic strain: threshold between 8% and 10%. The line is a guideline to the eye only in accordance to the Avrami model.

as well as displaced Mn atoms go to vacant Ga sites". However, it is to be noted that grain growth is observed at temperatures as high as 1000 °C which is above the $L2_1$ ordering temperature while we could only compare the defect concentrations of the alloys at room temperature. Therefore, we cannot exclude a different concentration of thermally activated vacancies of the alloys.

Still, another origin for the hindered grain growth in some alloys could be less mobile (possibly pinned) grain boundaries. For this purpose experiments aiming at the activation of the grain boundary motion were performed, i.e. the $Ni_{50}Mn_{29}Ga_{21}$ samples were hot deformed. The following procedure was applied: The samples were heated up to 1000 °C within approximately 30 min. After a dwell time of 15 min they were compressed at a constant strain rate of $1 \times 10^{-4}\,s^{-1}$ to a reduction in height of 6%, 8%, 10%, 15% and 17%, respectively. After deformation, each sample was kept at 1000 °C for further 6 h without external load.

Fig. 5 shows the microstructures of the samples after hot deformation and annealing for an applied strain of 6%, 10% and 17%, respectively. The samples, which were deformed by 6% and 8% prior to annealing show a fine grained microstructure with twin boundaries in almost every grain and no particular grain growth. In contrast, the sample strained by 10% reveals large grains of the dimension of the sample diameter. Similar results were obtained for samples, which were deformed by 15% and 17%. No further grain growth was observed with increasing strain. Thus, for the composition $Ni_{50}Mn_{29}Ga_{21}$ at 1000 °C grain growth can be initiated by hot deformation of at least 10%. In Fig. 6 the average grain size in dependence of the plastic strain can be seen. It clearly shows a threshold for grain growth at a strain level between 8% and 10%. Thus, we conclude that a distinct activation is necessary to induce grain growth. Once the grain growth has been initiated, no significant obstacles are present and grain growth is only stopped at the sample surface. Hence, the hindered grain growth in $Ni_{50}Mn_{29}Ga_{21}$ can be attributed to grain boundary pinning. Measuring the grain orientation by X-ray diffraction in a 4-circle diffractometer did not reveal a correlation between the compression direction and the grain orientation.

4. Summary

The influence of different annealing temperatures and times on the microstructure of Ni–Mn–Ga alloys was investigated. The compositions of these alloys include $Ni_{50}Mn_{29}Ga_{21}$, a magnetic shape memory alloy, being active at room temperature, and $Ni_{48}Mn_{30}Ga_{22}$ which is investigated as a reference material. Above 1000 °C grain growth occurred in $Ni_{48}Mn_{30}Ga_{22}$. In contrast $Ni_{50}Mn_{29}Ga_{21}$ shows no grain growth up to the melting temperature. Increasing the annealing time neither led to a stronger grain growth in $Ni_{48}Mn_{30}Ga_{22}$ nor initiated grain growth in $Ni_{50}Mn_{29}Ga_{21}$. In order to clarify the influence of the room temperature structure and the Ni-content on the occurrence of grain growth further alloys ($Ni_{49}Mn_{30}Ga_{21}$, $Ni_{50}Mn_{25}Ga_{25}$ and $Ni_{51}Mn_{29}Ga_{21}$) were investigated. Hereby, only alloys with a Ni-content below 50 at.% showed grain growth.

Two different origins for the different grain growth behavior were considered: (1) the assumption of the existence of constitutional vacancies in $Ni_{48}Mn_{30}Ga_{22}$ in comparison to $Ni_{50}Mn_{29}Ga_{21}$ could be excluded by PAS measurements. Thus, the grain growth in $Ni_{48}Mn_{30}Ga_{22}$ is not initiated by constitutional vacancies. (2) Assuming a restricted grain boundary mobility we attempted to release the grain boundaries by hot deformation and subsequent annealing. Here, deformation and annealing at 1000 °C showed that a critical deformation of about 10% is necessary to initiate grain growth, which remains unhindered until the sample surface is reached. Hence, activation is required to initiate grain growth in $Ni_{50}Mn_{29}Ga_{21}$.

Therefore, we can conclude that the different grain growth behavior in Ni–Mn–Ga alloys is due to grain boundary pinning for alloys with a Ni-content of 50% or above. The origin of the pinning will be object of a future study.

Acknowledgements

The authors kindly acknowledge financial support by the German Science Foundation (DFG) code RO962/5.

References

[1] A. Sozinov, A.A. Likachev, N. Lanska, K. Ullakko, Appl. Phys. Lett. 80 (2002) 1746–1748.
[2] M.A. Marioni, R.C. O'Handley, S.M. Allen, J. Magn. Magn. Mater. 290 (2005) 1966–1968.
[3] I. Suorsa, E. Pagounis, K. Ullakko, Appl. Phys. Lett. 84 (2004) 4658–4660.
[4] M. Pasquale, Sens. Actuators A: Phys. 106 (2003) 142–148.
[5] M. Frommberger, M. Tewes, A. Ludwig, Ch. Zanke, E. Quandt, Trans. Magn. Soc. Jpn. 3 (2005) 115–117.
[6] V.A. Chernenko, E. Cesari, V.V. Kokorin, I.N. Vitenko, Scripta Metall. Mater. 33 (1995) 1239–1244.
[7] K. Ullakko, J.K. Huang, C. Kantner, R.C. O'Handley, V.V. Kokorin, Appl. Phys. Lett. 69 (1996) 1966–1968.
[8] C. Jiang, J. Liu, J. Wang, L. Xu, H. Xu, Acta Mater. 53 (2005) 1111–1120.
[9] M. Pötschke, U. Gaitzsch, S. Roth, B. Rellinghaus, L. Schultz, J. Magn. Magn. Mater. 316 (2007) 383–385.
[10] U. Gaitzsch, M. Pötschke, S. Roth, B. Rellinghaus, L. Schultz, Scripta Mater. 57 (2007) 493–495.
[11] U. Gaitzsch, M. Pötschke, S. Roth, B. Rellinghaus, L. Schultz, Acta Mater. 57 (2009) 365–370.
[12] U. Gaitzsch, M. Pötschke, S. Roth, N. Mattern, B. Rellinghaus, L. Schultz, J. Alloy Compd. 443 (2007) 99–104.
[13] D.L. Schlagel, R.W. McCallum, T.A. Lograsso, J. Alloy Compd. 463 (2008) 38–46.
[14] W.M. Yuhasz, D.L. Schlagel, Q. Xing, K.W. Dennis, R.W. McCallum, T.A. Lograsso, J. Appl. Phys. 105 (2009), 07A921-1–07A921-3.
[15] J. Liu, M. Xia, Y. Huang, H. Zheng, J. Li, J. Alloy Compd. 417 (2006) 96–99.
[16] J. Liu, H. Xie, J. Li, J. Cryst. Growth 300 (2007) 272–276.
[17] X. Jin, M. Marioni, S.M. Allen, R.C. O'Handley, J. Appl. Phys. 91 (2002) 8222–8224.
[18] W. Brandt, A. Dupasquier, Proceedings of the International School of Physics "Enrico Fermi", North-Holland Publishing Company, Amsterdam/New York/Oxford, 1983.
[19] R.W. Overholser, M. Wuttig, D.A. Neumann, Scripta Mater. 40 (1999) 1095–1102.
[20] M.L. Richard, J. Feuchtwanger, S.M. Allen, R.C. O'Handley, P. Lazpita, J.M. Barandiaran, J. Gutierrez, B. Ouladdiaf, C. Mondelli, T. Lograsso, D. Schlagel, Philos. Mag. 87 (2007) 3437–3447.